

# Polaron coupling constants in BaSnO<sub>3</sub>

Christian A. Niedermeier<sup>1,2,a</sup>, Toshio Kamiya<sup>2,3</sup>, Michelle A. Moram<sup>1</sup>

<sup>1</sup>Department of Materials, Imperial College London, Exhibition Road, London, SW7 2AZ, UK

<sup>2</sup>Laboratory for Materials and Structures, Tokyo Institute of Technology, Mailbox R3-4, 4259 Nagatsuta, Midori-ku, Yokohama, 226-8503, Japan

<sup>3</sup>Materials Research Center for Element Strategy, Tokyo Institute of Technology, 4259 Nagatsuta, Midori-ku, Yokohama, 226-8503, Japan

**Abstract:** The transverse and longitudinal optical phonon modes in BaSnO<sub>3</sub> are re-evaluated from the previously reported far-infrared ellipsometry spectra of single crystals. These are employed to determine polaron coupling constants, which provide the basis for theoretical calculations of the room temperature electron mobility in BaSnO<sub>3</sub>. The relaxation time for the longitudinal optical phonon scattering in BaSnO<sub>3</sub> is larger as compared to SrTiO<sub>3</sub>, contributing to the high room temperature electron mobility reported for the La-doped BaSnO<sub>3</sub> single crystals.

arXiv:1612.01343v1 [cond-mat.mtrl-sci] 5 Dec 2016

---

<sup>a</sup>Corresponding author, e-mail: c.niedermeier13@imperial.ac.uk

Single crystals of the transparent perovskite La-doped  $\text{BaSnO}_3$  have recently attracted significant attention due to the unprecedented high room temperature mobility of  $320 \text{ cm}^2/\text{Vs}$  [1], which is the highest value reported for perovskite oxides. A fundamental understanding of the superior electron transport in  $\text{BaSnO}_3$  is of immediate importance for applications in oxide electronics. Due to advanced vapour phase epitaxy methods, the electron mobility limit is now dictated by the intrinsic physical properties of the material rather than determined by the defects associated with thin film crystal growth. In addition, the discovery of a high mobility electron gas at perovskite oxide heterointerfaces [2] promotes a new design of electronic devices in which unordinary high carrier densities are realized and consequently high mobility electron transport is attained without scattering by electron-impurity interactions induced by substitutional doping.

The high mobility in  $\text{BaSnO}_3$  stems from the large dispersion of the conduction band comprised of Sn 5s orbitals [3], yielding a small electron effective mass of only  $m_e^* = 0.19 m_0$  [4]. Furthermore, the large static dielectric constant of  $\epsilon_s = 20$  [5] promotes the screening of defects such as dislocations and ionized impurities [4, 6], and the small density of states of the conduction band singly-degenerated at the  $\Gamma$  point of the Brillouin zone reduces the longitudinal optical (LO) phonon scattering rate [7], both resulting in an unusually high mobility as compared to many other established transparent conducting oxides. An accurate first-principles theoretical calculation of the electron-phonon interactions in  $\text{BaSnO}_3$  requires a significant computational effort, in particular when the La doping effect on the conduction band dispersion is taking into account requiring large supercells. Therefore, this work determines the polaron coupling constants for  $\text{BaSnO}_3$  from experimental results to provide a valuable basis for calculation of the mobility governed by electron-phonon interactions. The relaxation time for LO phonon scattering in  $\text{BaSnO}_3$  is about twice as large as compared to  $\text{SrTiO}_3$ , supporting a high electron mobility at room temperature.

To calculate the polarizations of the transverse optical (TO) and LO phonon modes in

BaSnO<sub>3</sub>, and to determine the electron-phonon coupling constants, the polaron theory described by Eagles [8] is used and the equations therein will be referred to as Eq. (E-X). Far-infrared (IR) ellipsometry spectra of BaSnO<sub>3</sub> single crystals were measured by Stanislavchuk et al. [5] in the frequency range of 50 – 680 cm<sup>-1</sup>. The previous work reported three optically IR-active TO phonon modes at frequencies of 135 (TO<sub>1</sub>), 245 (TO<sub>2</sub>) and 628 cm<sup>-1</sup> (TO<sub>3</sub>), and the corresponding absorption strengths. However, reproduction of the IR dielectric function shows that the reported LO phonon frequencies do not accurately coincide with the maxima of the loss function  $-\text{Im}(\varepsilon^{-1}(\omega))$  and also the TO<sub>2</sub> phonon absorption strength is slightly underestimated with the given parameter set. Thus the dielectric function is reprinted from Ref. [5] for re-evaluation in this work (Fig. 1). Due to the small BaSnO<sub>3</sub> crystal size, light scattering effects result in an artificial decrease of the real part of the dielectric function  $\varepsilon_1(\omega)$  and an increase in the imaginary part of the dielectric function  $\varepsilon_2(\omega)$  below a frequency of 150 cm<sup>-1</sup>.

The optical spectra are fitted by a least squares method using a model comprised of three Lorentz oscillators for the different phonon modes ( $\mu = 1, 2, 3$ ) in the frequency range 150 to 680 cm<sup>-1</sup>

$$\epsilon(\omega) = \varepsilon_\infty + \sum_{\mu} \frac{A_{\mu}\omega_{t_{\mu}}^2}{\omega_{t_{\mu}}^2 - \omega^2 - i\gamma_{\mu}\omega} \quad (1)$$

where  $\varepsilon_\infty$  is the high frequency dielectric constant,  $A_{\mu}$  is the absorption strength,  $\omega_{t_{\mu}}$  is TO phonon mode frequency and  $\gamma_{\mu}$  is the broadening frequency. The LO phonon frequencies are determined from the maxima of the loss function  $-\text{Im}(\varepsilon(\omega)^{-1})$  and all parameters are summarized in Tab. III. The static dielectric constant  $\varepsilon_s = 20 \pm 2$  is calculated by the sum of the high frequency dielectric constant and the low frequency limits of all the phonon dielectric constants, according to  $\varepsilon_s = \varepsilon_\infty + \sum_{\mu} A_{\mu}$ .

The polarization  $p_{t_{\mu}}$  associated with each TO phonon mode is calculated according to Eq. (E-4) [8, 9]

$$p_{t_{\mu}}^2 = \frac{A_{\mu}\omega_{t_{\mu}}^2}{4\pi N} \quad (2)$$

where  $N$  denotes the number of unit cells per volume (Table II). The polarization  $p_{1\mu}$

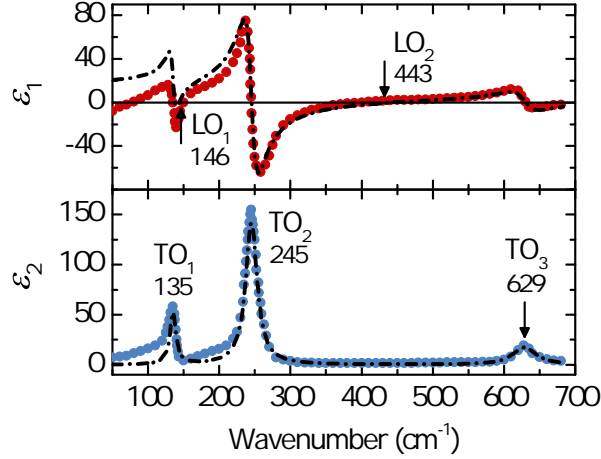


FIG. 1: Real (red) and imaginary (blue) parts of the BaSnO<sub>3</sub> dielectric function  $\varepsilon(\omega)$  recorded with far-IR spectroscopic ellipsometry of a single crystal, reprinted from Stanislavchuk et al., J. Appl. Phys. **112**, 044108 (2012) [5] with the permission of AIP Publishing. Black dashed lines indicate the fit to the dielectric function  $\varepsilon(\omega)$  using three Lorentz oscillators with parameters given in Table I. The TO phonon modes are given by the absorption modes indicated by the maxima of the imaginary part of the dielectric function  $\varepsilon_2(\omega)$ . The maxima of the loss function  $-\text{Im}(\varepsilon^{-1}(\omega))$  determine the LO phonon modes near  $\varepsilon_1(\omega) = 0$ .

associated with each of the LO phonon modes is calculated according to Eqs. (E-7, E-8)

$$p_{l_{\mu'}}^2 \sum_{\mu} \left( \frac{p_{t_{\mu}}}{\omega_{t_{\mu}}^2 - \omega_{l_{\mu'}}^2} \right)^2 = \left( \frac{\varepsilon_{\infty}}{4\pi N} \right)^2. \quad (3)$$

The polaron coupling constants  $\alpha_{\mu}$  are calculated according to Eq. (E-27)

$$\alpha_{\mu} = \frac{e^2}{r_{\mu} \hbar \omega_{l_{\mu}}} \frac{f_{\mu}^2}{8\pi \varepsilon_0} \left( \frac{1}{\varepsilon_{\infty}} - \frac{1}{\varepsilon_s} \right) \quad (4)$$

where  $e$  is the electron charge,  $\hbar$  is the reduced Planck constant and  $\varepsilon_0$  is the vacuum dielectric constant. The parameter  $f_{\mu}^2$  is defined by Eq. (E-23)

$$f_{\mu}^2 = \frac{p_{l_{\mu}}^2 / \omega_{l_{\mu}}^2}{\sum_{\mu} p_{l_{\mu}}^2 / \omega_{l_{\mu}}^2} \quad (5)$$

TABLE I: TO and LO phonon modes in BaSnO<sub>3</sub> obtained by modelling three Lorentz oscillators to the IR dielectric function measured by spectroscopic ellipsometry. The broadening frequency  $\gamma_\mu$  and absorption strength  $A_\mu$  ( $\mu = 2, 3$ ) were used as fitting parameters. The static and high frequency dielectric constants are  $\epsilon_s = 20 \pm 2$  and  $\epsilon_\infty = 3.3$  [5], respectively.

Mode	Phonon frequency		Broadening frequency	Absorption strength
$\mu$	$\omega_{t_\mu}$	$\omega_{l_\mu}$	$\gamma_\mu$	$A_\mu$
	(cm <sup>-1</sup> )	(cm <sup>-1</sup> )	(cm <sup>-1</sup> )	-
1	135 <sup>a</sup>	146	10 <sup>a</sup>	3.8 <sup>a</sup> $\pm$ 2
2	245 <sup>a</sup>	443	20	11.4
3	629 <sup>a</sup>	784	39	1.1

<sup>a</sup>Reference [5].

and the polaron radius  $r_\mu$  is defined by Eq. (E-29)

$$r_\mu = \left( \frac{\hbar}{2m_e^* \omega_{l_\mu}} \right)^{1/2} \quad (6)$$

where  $m_e^*$  is the electron effective mass and  $m_0$  is the electron rest mass. The calculated polaron coupling constants  $\alpha_\mu$  for all LO phonon modes in BaSnO<sub>3</sub> and SrTiO<sub>3</sub> are summarized in Table IV.

Based on the electron effective mass of  $m_e^* = 0.19 m_0$  for BaSnO<sub>3</sub> [4] and  $m_e^* = 1.8 m_0$  for SrTiO<sub>3</sub> [11], the relaxation times  $\tau_\mu$  for the corresponding phonon scattering modes were calculated according to [13, 14]

$$\tau_\mu = \frac{1}{2\alpha_\mu \omega_{l_\mu}} \left( 1 + \frac{\alpha_\mu}{6} \right)^{-2} f(\alpha_\mu) \left( \exp \left( \frac{\hbar \omega_{l_\mu}}{k_B T} \right) - 1 \right) \quad (7)$$

where  $k_B$  is the Boltzmann constant,  $T$  is the absolute temperature and  $f(\alpha_\mu)$  is a slowly varying function ranging from 1.0 to 1.2 for  $0 < \alpha_\mu < 3$  [15]. The effective carrier relaxation

TABLE II: Number of unit cells per unit volume  $N$ , static and high frequency dielectric constants  $\varepsilon_s$  and  $\varepsilon_\infty$ , electron effective mass  $m_e^*$  of BaSnO<sub>3</sub> and SrTiO<sub>3</sub>. Parameters are used to calculate the polarizations associated with each phonon mode, the polaron coupling constants and the relaxation time of carrier scattering by LO phonons.

Material	Unit cells/volume	Dielectric constants		Electron effective mass
	$N$ (cm <sup>-3</sup> )	$\varepsilon_s$	$\varepsilon_\infty$	$m_e^*$ ( $m_0$ )
BaSnO <sub>3</sub>	$1.43 \cdot 10^{22}$	20 <sup>a</sup>	3.3 <sup>a</sup>	0.19 <sup>b</sup>
SrTiO <sub>3</sub>	$1.68 \cdot 10^{22}$	310 <sup>c</sup>	5.2 <sup>c</sup>	1.8 <sup>d</sup>

<sup>a</sup>Reference [5].

<sup>b</sup>Reference [4].

<sup>c</sup>Reference [10].

<sup>d</sup>Reference [11].

time  $\tau_{\text{eff}}$  for LO phonon scattering in each material is calculated according to [8]

$$\tau_{\text{eff}}^{-1} = \sum_{\mu} \tau_{\mu}^{-1}, \quad (8)$$

and is predominantly determined by the smallest value of relaxation time  $\tau_{\mu}$  among all LO phonon modes. Since the relaxation time denotes the average time of momentum loss by scattering to electron-phonon interactions, a high electron mobility  $\mu_e$  may be expected when the relaxation time is large, according to [16]

$$\mu_e = \frac{e\tau_{\text{eff}}}{m_e^*}. \quad (9)$$

While the SrTiO<sub>3</sub> mobility at cryogenic temperatures may be as large as 32 000 cm<sup>2</sup>/Vs [17], the room temperature mobility does not exceed 10 cm<sup>2</sup>/Vs [18] mainly as a result of the small carrier relaxation time  $\tau_3 = 2.6 \times 10^{-14}$  s for the LO<sub>3</sub> phonon scattering mode with the energy  $\hbar\omega_{l_3} = 99$  meV (Fig. 2) and the large electron effective mass  $m_e^* = 1.8 m_0$  [11]. It is striking to observe that the BaSnO<sub>3</sub> room temperature mobility

TABLE III: TO and LO phonon modes in BaSnO<sub>3</sub> and SrTiO<sub>3</sub>, where  $p_{\beta_{\mu}}$  denotes the corresponding polarization calculated according to Eq. (2).

Material	Mode	Frequency	Energy	Absorption strength		
	$\beta_{\mu}$	$\omega_{\beta_{\mu}}$	$\hbar\omega_{\beta_{\mu}}$	$A_{\mu}$	$p_{\beta_{\mu}}^2 / \sum_{\mu} p_{\beta_{\mu}}^2$	$\sum_{\mu} p_{\beta_{\mu}}^2$
		(cm <sup>-1</sup> )	(meV)	-	-	(cm <sup>3</sup> s <sup>-2</sup> )
BaSnO <sub>3</sub>	t <sub>1</sub>	135 <sup>a</sup>	17	3.8 <sup>a</sup>	0.07	
	t <sub>2</sub>	245 <sup>a</sup>	30	11	0.50	2.3 · 10 <sup>5</sup>
	t <sub>3</sub>	629 <sup>a</sup>	78	1.1	0.43	
	l <sub>1</sub>	146	18	-	0.001	
	l <sub>2</sub>	443	55	-	0.19	2.3 · 10 <sup>5</sup>
	l <sub>3</sub>	784	97	-	0.81	
SrTiO <sub>3</sub>	t <sub>1</sub>	88 <sup>b</sup>	11	300 <sup>b</sup>	0.80	
	t <sub>2</sub>	178 <sup>b</sup>	22	3.6 <sup>b</sup>	0.04	4.8 · 10 <sup>5</sup>
	t <sub>3</sub>	544 <sup>b</sup>	67	1.6 <sup>b</sup>	0.16	
	l <sub>1</sub>	172 <sup>b</sup>	21	-	0.0003	
	l <sub>2</sub>	469 <sup>b</sup>	58	-	0.07	4.8 · 10 <sup>5</sup>
	l <sub>3</sub>	798 <sup>b</sup>	99	-	0.93	

<sup>a</sup>Reference [5].

<sup>b</sup>Reference [10],  $\omega_{1_{\mu}}$  recalculated from the loss function  $-\text{Im}(\varepsilon(\omega)^{-1})$ .

TABLE IV: Polaron coupling constants  $\alpha_\mu$  according to Eq. (4) for different LO phonon modes in BaSnO<sub>3</sub> and SrTiO<sub>3</sub>. The parameter  $f_\mu^2$  and the polaron radius  $r_\mu$  are defined by Eqs. (5) and (6), respectively.

Material	Mode	Energy $\hbar\omega_{l_\mu}$ (meV)	Polaron coupling const.			
			$f_\mu^2$ -	$r_\mu \left(\frac{m_e^*}{m_0}\right)^{0.5}$ (Å)	$\alpha_\mu \left(\frac{m_0}{m_e^*}\right)^{0.5}$ -	$\alpha_\mu$ -
BaSnO <sub>3</sub>	$l_1$	18	0.03	14.5	0.18	0.08
	$l_2$	55	0.41	8.3	1.61	0.70
	$l_3$	97	0.57	6.3	1.70	0.74
SrTiO <sub>3</sub> <sup>a</sup>	$l_1$	21	0.005	13.4	0.03	0.03
	$l_2$	58	0.18	8.1	0.51	0.69
	$l_3$	99	0.82	6.2	1.81	2.43

<sup>a</sup>cf. Reference [12].



is predominantly determined by the LO<sub>2</sub> phonon mode with the energy  $\hbar\omega_{1_2} = 55$  meV, resulting in a larger relaxation time of  $\tau_2 = 4.7 \times 10^{-14}$  s.

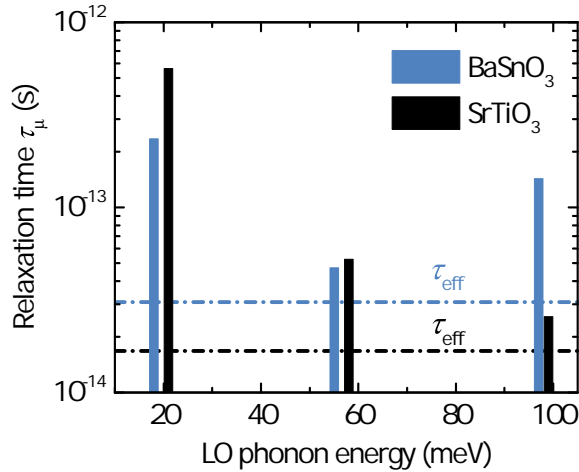


FIG. 2: Relaxation time of carrier scattering by LO phonons calculated for BaSnO<sub>3</sub> (blue) and SrTiO<sub>3</sub> (black). The effective scattering relaxation time  $\tau_{\text{eff}} = 1/\sum_{\mu}\tau_{\mu}^{-1}$  for each material is given by the dashed lines.

As compared to SrTiO<sub>3</sub>, the enhanced  $\sim 300$  cm<sup>2</sup>/Vs room temperature mobility achievable in La-doped BaSnO<sub>3</sub> single crystals [1] is thus attributed to the larger effective carrier relaxation time as well as the significantly smaller electron effective mass of  $m_e^* = 0.19 m_0$  [4].

In summary, the BaSnO<sub>3</sub> polaron coupling constants were calculated based on previously reported experimental far-IR reflectivity spectra to provide the basis for a facile calculation of the mobility governed by LO phonon scattering. The enhanced room temperature mobility in La-doped BaSnO<sub>3</sub> single crystals results from the larger relaxation time for carrier scattering as well as the comparably small electron effective mass.

## Acknowledgements

We are thankful to Dr T. Stanislavchuk for discussion of the BaSnO<sub>3</sub> IR ellipsometry spectra. C. A. Niedermeier and M. A. Moram acknowledge support from the Leverhulme Trust via M. A. Moram's Research Leadership Award (RL-0072012). M. A. Moram acknowledges further support from the Royal Society through a University Research Fellowship. The work at Tokyo Institute of Technology was supported by the Ministry of Education, Culture, Sports, Science and Technology (MEXT) Element Strategy Initiative to Form Core Research Center.

## References

- [1] H. J. Kim, U. Kim, H. M. Kim, T. H. Kim, H. S. Mun, B.-G. Jeon, K. T. Hong, W.-J. Lee, C. Ju, K. H. Kim, and K. Char, *Applied Physics Express* **5**, 061102 (2012).
- [2] A. Ohtomo and H. Y. Hwang, *Nature* **427**, 423 (2004).
- [3] H. Mizoguchi, H. W. Eng, and P. M. Woodward, *Inorganic Chemistry* **43**, 1667 (2004).
- [4] C. A. Niedermeier, S. Rhode, K. Ide, H. Hiramatsu, H. Hosono, T. Kamiya, and M. A. Moram, arXiv:1609.05508 (2016).
- [5] T. N. Stanislavchuk, A. A. Sirenko, A. P. Litvinchuk, X. Luo, and S.-W. Cheong, *Journal of Applied Physics* **112**, 044108 (2012).
- [6] H. J. Kim, U. Kim, T. H. Kim, J. Kim, H. M. Kim, B.-G. Jeon, W.-J. Lee, H. S. Mun, K. T. Hong, J. Yu, K. Char, and K. H. Kim, *Phys. Rev. B* **86**, 165205 (2012).
- [7] K. Krishnaswamy, B. Himmetoglu, Y. Kang, A. Janotti, and C. G. V. de Walle, arXiv:1610.06253 (2016).
- [8] D. M. Eagles, *Journal of Physics and Chemistry of Solids* **25**, 1243 (1964).

- [9] T. Kurosawa, *Journal of the Physical Society of Japan* **16**, 1298 (1961).
- [10] W. G. Spitzer, R. C. Miller, D. A. Kleinman, and L. E. Howarth, *Phys. Rev.* **126**, 1710 (1962).
- [11] M. Ahrens, R. Merkle, B. Rahmati, and J. Maier, *Physica B: Condensed Matter* **393**, 239 (2007).
- [12] D. M. Eagles, *Journal of Physics and Chemistry of Solids* **26**, 672 (1965).
- [13] H. Fröhlich and N. F. Mott, *Proceedings of the Royal Society of London A: Mathematical, Physical and Engineering Sciences* **171**, 496 (1939).
- [14] F. E. Low and D. Pines, *Phys. Rev.* **91**, 193 (1953).
- [15] F. E. Low and D. Pines, *Phys. Rev.* **98**, 414 (1955).
- [16] R. E. Hummel. *Electronic Properties of Materials*. Springer-Verlag New York, 4th edition, (2011).
- [17] J. Son, P. Moetakef, B. Jalan, O. Bierwagen, N. J. Wright, R. Engel-Herbert, and S. Stemmer, *Nat Mater* **9**, 482 (2010).
- [18] A. Verma, A. P. Kajdos, T. A. Cain, S. Stemmer, and D. Jena, *Phys. Rev. Lett.* **112**, 216601 (2014).